

# Harnessing Creative Methods for EEG Feature Extraction and Modeling in Neurological Disorder Diagnoses

Avish Jha

*School of Comp. Sci. & Eng. Vellore Institute of Technology Vellore, India*  
avish.j@protonmail.com

Nevin Kuruvilla

*School of Comp. Sci. & Eng. Vellore Institute of Technology Vellore, India*  
nevinmathewsk@gmail.com

Pramika Garg

*School of Comp. Sci. & Eng. Vellore Institute of Technology Vellore, India*  
micepram@gmail.com

Dr. Akila Victor

*School of Comp. Sci. & Eng. Vellore Institute of Technology Vellore, India*  
akilavictor@vit.ac.in

**Abstract**—Amidst the rising incidence of neurological disorders detected through electroencephalograms (EEG), this study explores innovative techniques for feature extraction. Analyzing EEG data from 88 subjects across 19 channels, a diverse set of 18 features including Relative Intensity Ratio, Power Spectral Intensity, Petrosian Fractal Dimensions, Hjorth Mobility, Hjorth Complexity, Detrended Fluctuation Analysis, Higuchi Fractal Dimension, Hjorth Activity, Sample Entropy, and Lempel-Ziv Complexity and many more are extracted. Encompassing temporal and spectral domains, these features provide comprehensive insights into neurophysiological processes, enabling nuanced EEG data exploration and identification of subtle patterns linked with various neurological disorders. Through rigorous analysis, we evaluate the efficacy of these features in precise disease discrimination using advanced building on two models: Bagging Blended Combination of XGBoost and LightGBM (BBE-XL) and a Multilayer Artificial Neural Network (ML-ANN). By deciphering intricate EEG signal information, this study aids in early detection and intervention for EEG-related disorders, with 97.62% accuracy.

**Index Terms**—EEG, XGBoost, LightGBM, ANN, Fractal Dimensions, Hjorth, Entropy

## I. INTRODUCTION

The field of neuroscience has experienced a remarkable transformation with the widespread adoption of electroencephalograms (EEG) as a pivotal tool for detecting, diagnosing, and monitoring various brain disorders [1]. EEG records the electrical activity of the brain by placing electrodes on the scalp, providing invaluable insights into the intricate neural processes that govern cognitive, sensory, and motor functions [2]. The real-time data provided by EEG can offer valuable insights into brainwave patterns, helping medical professionals assess brain health and aiding in the formulation of appropriate treatment strategies. Additionally, EEG's non-invasive nature and high temporal resolution make it a valuable tool for understanding the brain's dynamic activity and its responses to different stimuli, contributing to our understanding of cognition, emotions, and neurological disorders.

In recent times, there has been a disconcerting upswing in the occurrence and prevalence of brain disorders, ranging from epileptic seizures, neurodegenerative conditions, to neu-

ropsychiatric ailments, a surge that can be ascribed to various interplaying factors such as the shifting demographics towards older populations, transformative lifestyle habits, heightened health consciousness, and advancements in diagnostic proficiency's. This concerning trend underscores a growing and urgent need for accurate, efficient, and scalable diagnostic tools; however, this surge in neurological disorders is paralleled by a shortage in the availability of specialized medical professionals capable of effectively diagnosing and managing these intricate conditions, necessitating the development of strategies to address this gap through bolstered medical education and innovative healthcare delivery approaches.

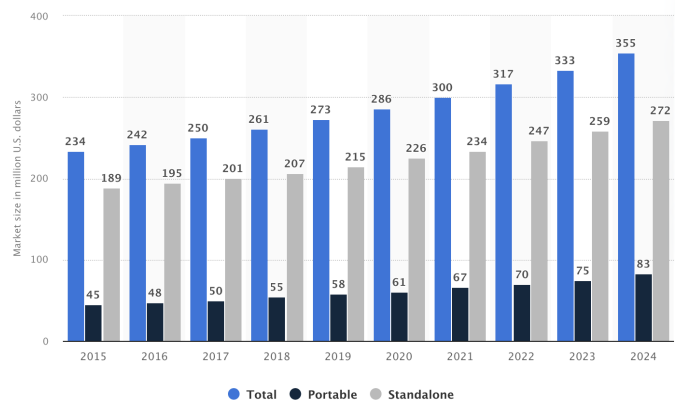


Fig. 1. US EEG Market from 2015 - 2024 [3]

As brain disorders become more prevalent, the healthcare sector faces challenges in providing timely and accurate diagnoses. The shortage is evident even in developed countries like the US, where there is a lack of EEG technicians despite the growing demand for EEG machines [4]. This can be evidently seen as even developed economies like the US are suffering a shortage of EEG technicians, with rising growth in EEG machine expansions as seen in Fig. 1 which was taken from [3]. To address these challenges, there's a crucial need for technologically advanced solutions that can assist medical practitioners in efficiently diagnosing and managing

brain disorders. These solutions could potentially bridge the gap between the increasing demand for neurological care and the limited availability of skilled professionals.

Before delving into our feature extraction and modeling methodologies, we glean insights from an extensive review of related literature. This synthesis illuminates the current landscape of EEG-based disease detection, highlighting the existing advancements, limitations, and potential research directions.

## II. LITERATURE SURVEY

In recent years, the domain of EEG analysis has witnessed a surge of interest in applying machine learning techniques for various bio-engineering applications. Ahi et al. [5] embarked on a comprehensive review spanning over three decades of literature (1988-2018), elucidating the diverse landscape of classification methods such as Naive-Bayes, Decision Tree/Random Forest, and Support Vector Machine (SVM). Notably, supervised methods like SVM and K-Nearest Neighbors (KNN) showcased superior accuracy compared to unsupervised counterparts. Interestingly, the potential for amalgamating these methods emerged as a strategy to enhance the overall classification accuracy, echoing the sentiments echoed by multiple studies in this domain.

A parallel endeavor by Ball et al. [6] delved into the realm of clinical EEG analysis, juxtaposing a feature-based framework against contemporary end-to-end methods. Their study drew upon the Temple University Hospital (TUH) Abnormal EEG Corpus (v2.0.0), encompassing a substantial dataset of around 3000 EEG recordings. Impressively, accuracy levels ranging from 81% to 86% were achieved across both the feature-based and end-to-end paradigms. The study's insights unveiled the significance of common data aspects such as delta and theta band power at specific temporal electrode locations, shared by both methodologies.

In the context of early prediction of epileptic seizures (ES), Rasheed et al. [7] offered a comprehensive review emphasizing the role of machine learning (ML) techniques, along with Deep Learning (DL) algorithms, in addressing this critical task. By thoroughly exploring facets like feature selection, ES detection, prediction, and evaluation methodologies, the study underscored the imminent importance of timely ES prediction. This review echoed the observations of Ahi et al. [5], revealing the potential of ML-based algorithms to revolutionize ES prediction, while also identifying gaps and challenges to inspire future investigations.

Drawing inspiration from similar themes, Rostami et al. [8] concentrated on diagnosing depression through nonlinear analysis of EEG signals. Their novel approach aimed to discern between depressed patients and normal subjects. Employing a diverse set of features, including power from EEG bands and four nonlinear metrics, the study harnessed classifiers like k-Nearest Neighbor, Linear Discriminant Analysis, and Logistic Regression. Results underscored the significance of feature combination, reminiscent of the insights from Ahi et al. [5], with the correlation dimension coupled with a

Logistic Regression classifier achieving the pinnacle accuracy of 83.3%. By integrating all nonlinear features with the Logistic Regression classifier, an accuracy of 90% was attained. This work illuminated the potential of combined features for enhanced performance.

Expanding on the realm of EEG-based Brain-Computer Interfaces (BCIs), Chugh et al. [9] conducted a comprehensive analysis of machine learning (ML) and deep learning (DL) techniques across various BCI frameworks, focusing on paradigms such as motor imagery, p300, and steady-state evoked potentials. Their survey not only highlighted ML's instrumental role in augmenting BCI efficiency but also addressed crucial challenges spanning signal processing, BCI functionality, performance assessment, and commercialization.

Mora et al. [10] introduced a novel multi-modal Machine Learning (ML) approach for classifying brain states based on EEG data. The approach creatively combined Continuous Wavelet Transform (CWT) and BiSpectrum (BiS) features, showcasing a resource-efficient alternative to deep learning methods. Notably, this approach focused on distinguishing between Mild Cognitive Impairment (MCI) and Alzheimer's disease (AD) patients from Healthy Control (HC) subjects. Their experimentation, employing a balanced dataset, showed the prowess of the concatenated CWT and BiS features (CWT+BiS) when coupled with the Multi-Layer Perceptron (MLP) classifier.

In line with the trajectory of employing EEG data for clinical insights, Mac et al. [11] devised a machine learning methodology to predict the effectiveness of selective serotonin reuptake inhibitor (SSRI) treatment in major depressive disorder (MDD) patients. Leveraging pre-treatment EEG data, their approach, which incorporated feature selection and a mixture of factor analysis (MFA) model, achieved a commendable accuracy of 87.9%, accompanied by promising specificity and sensitivity values.

Finally, Rami et al. [12] embarked on an extensive exploration of signal processing techniques within the realm of brain-computer interfaces (BCIs) involving motor movement classification. Employing a variety of machine learning algorithms, they harnessed features extracted from EEG signals to enhance classification accuracy, akin to the methodologies discussed in [5], [10].

Noteworthy achievements were observed, particularly with the Medium-ANN model, which demonstrated exceptional performance metrics such as AUC (Area Under Curve), Cohen's Kappa coefficient, Matthews correlation coefficient, and loss. These outcomes exemplified the versatility and applicability of the approach in scenarios ranging from robotic prostheses to resource-constrained environments.

In conclusion, the literature survey encapsulates the evolution of machine learning techniques in EEG analysis for bio-engineering applications. While various models and methodologies have been tested across different studies, the emphasis on feature extraction methods seems to have been relatively subdued.

Instead, a predominant trend emerges, where several papers

have leaned towards utilizing a limited set of fundamental features. This observation highlights an avenue for future exploration and underscores the potential of incorporating more advanced feature extraction techniques for further enhancements in EEG-based applications.

### III. METHODOLOGY

#### A. Data

This study employs an EEG dataset [13]–[15] with resting state-closed eyes recordings from 88 subjects, categorized into distinct groups: 36 with Alzheimer's disease (AD group), 23 with Frontotemporal Dementia (FTD group), and 29 healthy controls (CN group). The Mini-Mental State Examination (MMSE) was used to assess cognitive impairment, yielding scores of 17.75 ( $sd=4.5$ ) for AD, 22.17 ( $sd=8.22$ ) for FTD, and 30 for CN. Age averages were 66.4 ( $sd=7.9$ ) for AD, 63.6 ( $sd=8.2$ ) for FTD, and 67.9 ( $sd=5.4$ ) for CN.

EEG recordings were conducted at the Second Dept. of Neurology at the AHEPA General Hospital, using a Nihon Kohden Electroencephalogram twentyone-hundred hardware with nineteen scalp electrodes and 2 reference electrodes according to the 10-20 system [15]. The recordings followed a standardized protocol with closed eyes and skin impedance below 5  $k\Omega$ . A sampling rate of 500 Hz and resolution of 10  $\mu V/mm$  were employed.

Recording parameters were optimized [14], including sensitivity ( $10 \mu V/mm$ ), time constant (0.3 s), and high-frequency filter (70 Hz). Recording durations were around thirteen minutes for AD with a minimum of 5.1, maximum of 21.3, twelve minutes for FTD with a minimum of 7.9, maximum of 16.9, and thirteen point eight minutes for CN with a minimum of 12.5, maximum of 16.5, totaling fourhundred eightyfive minutes of AD, about two hundred seventysix minutes of FTD, and four hundred two minutes of CN recordings.

EEG preprocessing involved transforming recordings into BIDS-accepted .set format. A comprehensive regimen included Butterworth band-pass filtering (0.5 to 45 Hz), referencing to A1-A2, and Artifact Subspace Reconstruction (ASR) [13]. Independent Component Analysis (ICA) generated 19 components mirroring original signals. The "ICLabel" routine in EEGLAB facilitated automated classification, rejecting components with "eye artifacts" or "jaw artifacts" [15], managing residual eye movement artifacts despite closed-eye conditions.

#### B. Features

In this study, we emphasize a comprehensive examination of several features that have frequently been under-explored in prior research investigations. Our analysis encompasses a total of 18 distinct features, meticulously selected for evaluation, which are outlined below with their importance mentioned in Figure 2.

1) *Relative Intensity Ratio (RIR)*: RIR evaluates the distribution of spectral power within distinct frequency bands in an EEG signal. It quantifies the ratio of power within a specific frequency range to the total power across all frequencies. This

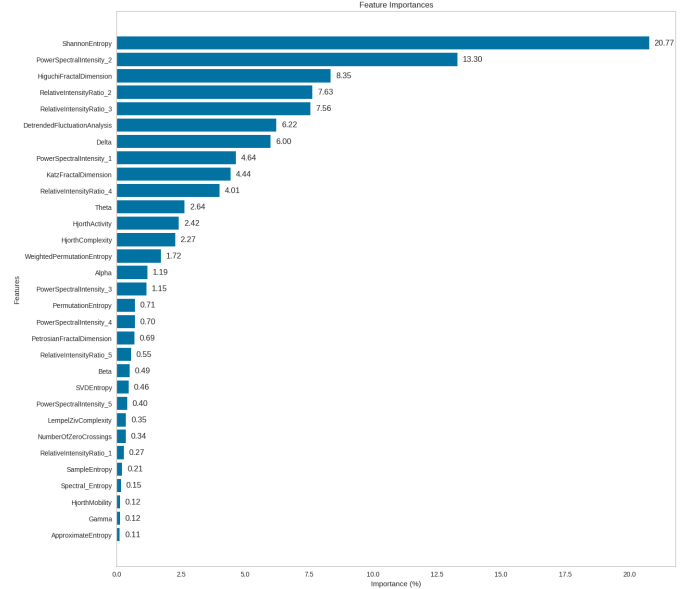


Fig. 2. Feature Importance

metric aids in identifying the dominance of certain frequency components.

$$RIR = \frac{\text{Power in Target Band}}{\text{Total Power}} \quad (1)$$

2) *Power Spectral Intensity (PSI)*: PSI characterizes the energy distribution across frequency bands within EEG data. By computing the power spectral density and integrating it within defined frequency ranges, PSI helps reveal the frequency-specific energy contributions. Here,  $P(f)$  is the power spectral density.

$$PSI = \int_{f_{\min}}^{f_{\max}} P(f) df, \text{ with } P(f) \quad (2)$$

3) *Petrosian Fractal Dimensions (PFD)*: PFD assesses the irregularity or fractal complexity of EEG waveforms across various scales.

$$PFD = \frac{\log_{10}(N)}{\log_{10}(N) + \log_{10}(\frac{N}{N+0.4N_{\text{peaks}}})} \quad (3)$$

4) *Hjorth Mobility*: Hjorth Mobility quantifies the abrupt changes in amplitude of an EEG signal, providing insight into its dynamic activity levels. Here,  $x$  is the EEG signal and  $\text{diff}$  represents the first discrete difference.

$$\text{Hjorth Mobility} = \frac{\text{stddev}(\text{diff}(x))}{\text{stddev}(x)} \quad (4)$$

5) *Hjorth Complexity*: Hjorth Complexity is a measure of EEG waveform complexity, indicating the irregularities in signal dynamics. It's derived by dividing Hjorth Mobility by the standard deviation of the first derivative, reflecting the interplay between signal mobility and its local variations.

$$\text{Hjorth Complexity} = \frac{\text{Hjorth Mobility}}{\frac{d}{dt}(\text{Hjorth Mobility})} \quad (5)$$

6) *Detrended Fluctuation Analysis (DFA)*: DFA investigates long-range correlations within EEG signals. It involves detrending the signal and calculating fluctuations to explore self-similarity. The calculation involves computing the root-mean-square of the integrated and detrended signal. Here,  $N$  is the signal length,  $y(i)$  represents the detrended signal, and  $\langle y \rangle_n$  is the local trend estimated over  $n$  data points.

$$DFA(n) = \sqrt{\frac{1}{N} \sum_{i=1}^N [y(i) - \langle y \rangle_n]^2}, \quad (6)$$

7) *Higuchi Fractal Dimension*: This dimension gauges temporal complexity in EEG data. It quantifies the relationship between signal length and the length of its trajectory on a 2D plane. Here,  $N$  is the signal length,  $r$  is the length of the sub-segments.

$$D = \frac{\log(N)}{\log(N/r)} \quad (7)$$

8) *Hjorth Activity*: Hjorth Activity characterizes the overall energy or amplitude variations within an EEG signal. It's determined by computing the variance of the signal and offers a glimpse into the general activity level of brain dynamics. Here,  $x$  is the EEG signal.

$$\text{Hjorth Activity} = \text{var}(x) \quad (8)$$

9) *Sample Entropy*: Sample Entropy evaluates the complexity of EEG signals by determining the likelihood of recurring patterns within a specified tolerance. It accommodates patterns of varying lengths [16]. The calculation involves comparing sequences of values with the designated tolerance. Here,  $A$  is the number of similar patterns of length  $m$  that are within a tolerance  $r$  of each other, and  $B$  is the number of similar patterns of length  $m + 1$  that are within the same tolerance  $r$ .

$$\text{Sample Entropy} = -\log \left( \frac{A}{B} \right) \quad (9)$$

10) *Lempel-Ziv Complexity*: Lempel-Ziv Complexity quantifies EEG signal complexity based on the minimal number of distinct patterns required for its representation. It employs the Lempel-Ziv compression algorithm. Here  $N$  is the embedding dimension,  $N!$  represents the factorial of  $N$ , and  $p_i$  is the probability of occurrence of the  $i$ th permutation.

$$\text{LZC} = \frac{\text{Number of Different Patterns}}{\text{Length of Signal}} \quad (10)$$

11) *Permutation Entropy*: Permutation entropy quantifies the complexity of a time series by measuring the diversity of its ordinal patterns. It characterizes the predictability of a signal based on the probabilities of observing different orderings of data points.

$$PE = -\sum_{i=1}^{N!} p_i \log_2(p_i) \quad (11)$$

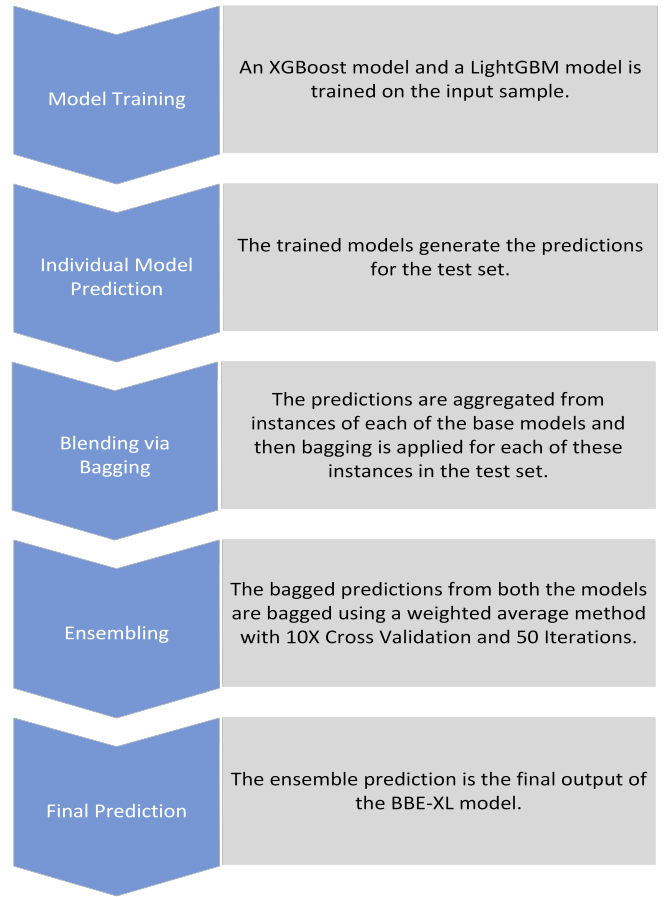


Fig. 3. Architecture of Bagging Blended Ensembled Combination of XGBoost and LightGBM (BBE-XL)

12) *Spectral Entropy*: Spectral entropy assesses the irregularity or complexity of the frequency distribution of an EEG signal's power spectrum [16]. It is a measure of the spread of energy across different frequency components. Here  $P(f)$  is the normalized power spectral density at frequency  $f$ .

$$SE = -\sum_f P(f) \log_2(P(f)) \quad (12)$$

13) *SVD Entropy*: Singular Value Decomposition (SVD) entropy quantifies the randomness or complexity of an EEG signal by considering the distribution of its singular values. It captures the level of variability and pattern richness in the signal. Here  $s_i$  is the  $i$ th singular value and  $N$  is the number of singular values.

$$SVD_{\text{Entropy}} = -\sum_{i=1}^N \frac{s_i}{\sum_{j=1}^N s_j} \log_2 \left( \frac{s_i}{\sum_{j=1}^N s_j} \right) \quad (13)$$

14) *Katz Fractal Dimension*: The Katz fractal dimension quantifies the complexity or self-similarity of an EEG signal's trajectory in phase space. It offers insights into the irregularity and fractal nature of the signal. Here  $L$  is the total length of

the signal's trajectory, and  $N$  is the length of the Euclidean distance between the first point in the trajectory and the point that maximizes it.

$$D_K = \frac{\log(L)}{\log(N/L)} \quad (14)$$

15) *Shannon Entropy*: Shannon entropy measures the uncertainty or information content of an EEG signal by considering the distribution of its amplitude values. It quantifies the level of randomness or disorder in the signal [16], [17]. Here  $n$  is the number of distinct amplitude values,  $x_i$  are the possible amplitude values, and  $p(x_i)$  is the probability of occurrence of  $x_i$ .

$$H(X) = - \sum_{i=1}^n p(x_i) \log_2 p(x_i) \quad (15)$$

16) *Weighted Permutation Entropy*: Weighted permutation entropy extends permutation entropy by assigning different weights to different ordinal patterns. It captures the significance of various patterns in the time series. Here  $w_i$  is the weight associated with the  $i$ th permutation.

$$WPE = - \sum_{i=1}^{N!} w_i \log_2(w_i) \quad (16)$$

17) *Approximate Entropy*: Approximate entropy quantifies the degree of regularity or similarity between sub-sequences within an EEG signal. It assesses how likely the signal is to remain close to its current state over successive time points [16], [17]. Here  $C_m(r)$  is the conditional probability that two sub-sequences of length  $m$  have a maximum difference less than  $r$  for a given  $m$  and tolerance  $r$ .

$$ApEn = - \log \left( \frac{C_{m+1}(r)}{C_m(r)} \right) \quad (17)$$

18) *Number of Zero Crossings*: The number of zero crossings indicates the frequency of oscillations or waveform changes in an EEG signal. It is used to estimate the signal's periodicity and dynamic behavior. Here  $N$  is the length of the signal and  $x_i$  are the signal values.

$$ZC = \frac{1}{2} \sum_{i=1}^{N-1} |\text{sign}(x_i) - \text{sign}(x_{i+1})| \quad (18)$$

Apart from the above mentioned features, Age, Gender and Mini-Mental State Examination (MMSE) were also used as Features, with the following models.

### C. Models

In this section, we present the two predictive models employed in this research: a Bagging Blended Ensembled Combination of XGBoost and LightGBM (BBE-XL) and a Multi-layer Artificial Neural Network (ML-ANN). These models were designed to address the complex and multifaceted nature of the prediction task, with each model leveraging distinct techniques to achieve optimal performance.

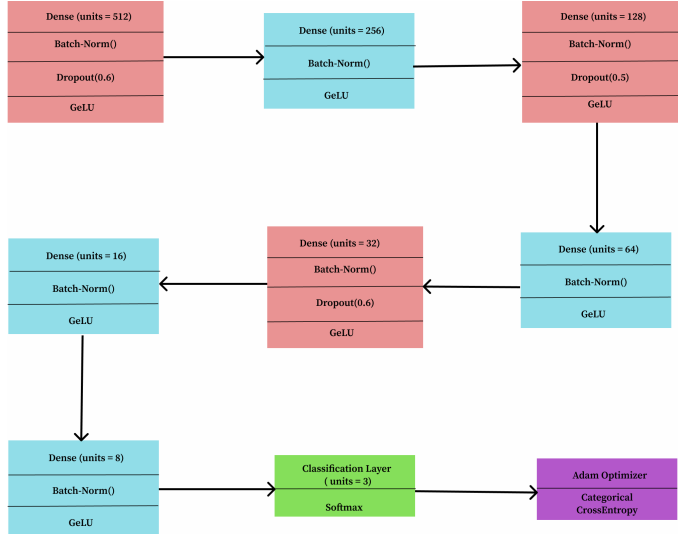


Fig. 4. Architecture of Multi-layer Artificial Neural Network (ML-ANN)

The BBE-XL is an ensemble model that amalgamates the strengths of two prominent gradient boosting frameworks, namely XGBoost and LightGBM. Bagging, a resampling technique, is employed to enhance the stability and generalizability of the ensemble. XGBoost and LightGBM models are trained on bootstrapped subsets of the training data, and their predictions are subsequently combined using a weighted averaging technique. Ensembling was further performed with 10 fold Cross Validation and 50 iterations for a total of 500 flows. By leveraging the complementary features of XGBoost and LightGBM, the BBE-XL model aims to mitigate overfitting while capturing intricate relationships within the data.

The Multilayer Artificial Neural Network (ML-ANN) constitutes a deep learning architecture tailored for intricate pattern recognition. Comprising multiple layers of interconnected neurons, the ML-ANN model is designed to capture intricate nonlinear relationships present in the data. The input layer accepts feature vectors, which are then propagated through hidden layers employing nonlinear activation functions. The network's weights are iteratively updated during training using backpropagation, optimizing predictive accuracy. Regularization techniques such as dropout are employed to prevent overfitting and enhance the model's generalization capability.

Both models undergo rigorous hyperparameter tuning to achieve optimal performance. The BBE-XL model's parameters, including learning rate, is fine-tuned using cross-validation. Similarly, the ML-ANN model's architecture, including the number of layers, neurons per layer, and activation functions, is optimized through a systematic search over hyperparameter space with 250 epochs.

## IV. RESULTS

To evaluate the models' predictive capabilities, a comprehensive suite of performance metrics is employed, encompassing accuracy, precision, recall, F1-score, and area under the

TABLE I  
MODEL RESULTS METRICS

Model	Performance Metrics					
	Accuracy	AUC	Recall	Precision	F1	Kappa
Multi-layer Artificial Neural Network (ML-ANN)	0.9761	0.982	0.9761	0.9765	0.9761	0.9631
Bagging Blended Ensembled Combination of XGBoost and LightGBM (BBE-XL)	0.9762	0.9970	0.9710	0.9766	0.9763	0.9635

receiver operating characteristic curve (AUC-ROC). Furthermore, extensive cross-validation and sensitivity analyses are performed to assess the models' robustness and generalizability, the results of which are given in Table I.

The obtained results for the Multilayer Artificial Neural Network (ML-ANN) and the Bagging Blended Ensembled Combination of XGBoost and LightGBM (BBE-XL) models remarkably demonstrate their exceptional performance in tackling the predictive task. Both models have showcased a remarkable level of accuracy, with ML-ANN achieving an accuracy of 0.9761 and BBE-XL achieving 0.9762. This marginal difference in accuracy between the two models signifies their comparable prowess in capturing complex patterns within the data. Additionally, the area under the curve (AUC) values for both models further substantiate their excellence, with ML-ANN achieving an AUC of 0.982 and BBE-XL closely following at 0.9970. This similarity in AUC underscores the models' robustness in distinguishing between different classes.

Moreover, when assessing the recall, precision, and F1-score metrics, both models continue to exhibit an outstanding degree of consistency. ML-ANN records a recall of 0.9761, while BBE-XL closely mirrors with a value of 0.9710. Likewise, precision values for ML-ANN (0.9765) and BBE-XL (0.9766) portray their capability to minimize false positives effectively. Notably, the F1-scores of 0.9761 for ML-ANN and 0.9763 for BBE-XL validate their adeptness in maintaining a harmonious balance between precision and recall.

## V. CONCLUSION

In this study, we presented two comprehensive methodologies for distinguishing EEG signals against two Electroencephalogram-Related Disorders: 'Alzheimers and Frontal-Dementia. Multiple features from frequency domain, entropy and fractal dimensions were computed to create the dataset. After this step, the curated dataset was implemented using the two models: Combination of XGBoost and LightGBM (BBE-XL) and a Multilayer Artificial Neural Network (ML-ANN) and both achieved an almost identical high accuracy of 97.61% & 97.62%.

This near-congruence in performance metrics not only accentuates the excellence of both models but also underscores their remarkable proximity in predictive capabilities. In conclusion, both the ML-ANN and BBE-XL models have exhibited commendable proficiency, with their consistently high performance across a spectrum of metrics establishing them as closely matched contenders in this predictive endeavor. This study shows how these algorithms can be a suitable helper for

reducing the burden on doctor's when diagnosing cognitive decline and other related diseases.

## REFERENCES

- [1] T. Kirschstein and R. Köhling, "What is the source of the EEG?," *Clinical EEG and Neuroscience*, vol. 40, no. 3, pp. 146–149, 2009. doi:10.1177/1550059409040000305
- [2] R. Elul, "The genesis of the EEG," *International Review of Neurobiology*, pp. 227–272, 1972. doi:10.1016/s0074-7742(08)60333-5
- [3] C. Stewart, "U.S. EEG market size by type 2015-2024," *Statista*, <https://www.statista.com/statistics/712730/us-eeg-market-size-projection-by-type/>
- [4] J. J. Majersik et al., "A shortage of neurologists – we must act now," *Neurology*, vol. 96, no. 24, pp. 1122–1134, 2021. doi:10.1212/wnl.00000000000012111
- [5] M.-P. Hosseini, A. Hosseini, and K. Ahi, "A review on machine learning for EEG signal processing in bioengineering," *IEEE Reviews in Biomedical Engineering*, vol. 14, pp. 204–218, 2021. doi:10.1109/rbme.2020.2969915
- [6] L. A. W. Gemein et al., "Machine-learning-based diagnostics of EEG Pathology," *NeuroImage*, vol. 220, p. 117021, 2020. doi:10.1016/j.neuroimage.2020.117021
- [7] K. Rasheed et al., "Machine learning for predicting epileptic seizures using EEG signals: A Review," *IEEE Reviews in Biomedical Engineering*, vol. 14, pp. 139–155, 2021. doi:10.1109/rbme.2020.3008792
- [8] B. Hosseiniard, M. H. Moradi, and R. Rostami, "Classifying depression patients and normal subjects using machine learning techniques and nonlinear features from EEG Signal," *Computer Methods and Programs in Biomedicine*, vol. 109, no. 3, pp. 339–345, 2013. doi:10.1016/j.cmpb.2012.10.008
- [9] S. Aggarwal and N. Chugh, "Review of machine learning techniques for EEG based brain computer interface," *Archives of Computational Methods in Engineering*, vol. 29, no. 5, pp. 3001–3020, 2022. doi:10.1007/s11831-021-09684-6
- [10] C. Ieracitano, N. Mammone, A. Hussain, and F. C. Morabito, "A novel multi-modal Machine Learning Based Approach for automatic classification of EEG Recordings in Dementia," *Neural Networks*, vol. 123, pp. 176–190, 2020. doi:10.1016/j.neunet.2019.12.006
- [11] A. Khodayari-Rostamabad, J. P. Reilly, G. M. Hasey, H. de Bruin, and D. J. MacCrimmon, "A machine learning approach using EEG data to predict response to SSRI treatment for major depressive disorder," *Clinical Neurophysiology*, vol. 124, no. 10, pp. 1975–1985, 2013. doi:10.1016/j.clinph.2013.04.010
- [12] F. J. Ramírez-Arias et al., "Evaluation of machine learning algorithms for classification of EEG Signals," *Technologies*, vol. 10, no. 4, p. 79, 2022. doi:10.3390/technologies10040079
- [13] A. Miltiadous et al., "A dataset of EEG recordings from: Alzheimer's disease, Frontotemporal dementia and Healthy subjects." *OpenNeuro*, 2023. doi:10.18112/openneuro.ds004504.v1.0.6
- [14] A. Miltiadous et al., "A dataset of scalp EEG recordings of alzheimer's disease, frontotemporal dementia and healthy subjects from routine EEG," *Data*, vol. 8, no. 6, p. 95, 2023. doi:10.3390/data8060095
- [15] A. Miltiadous, E. Gionanidis, K. D. Tzimourta, N. Giannakeas, and A. T. Tzallas, "Dice-Net: A novel convolution-transformer architecture for alzheimer detection in EEG Signals," *IEEE Access*, vol. 11, pp. 71840–71858, 2023. doi:10.1109/access.2023.3294618
- [16] A. Delgado-Bonal and A. Marshak, "Approximate entropy and sample entropy: A comprehensive tutorial," *Entropy*, vol. 21, no. 6, p. 541, 2019. doi:10.3390/e21060541
- [17] B. Bein, "Entropy," *Best Practice & Research Clinical Anaesthesiology*, vol. 20, no. 1, pp. 101–109, 2006. doi:10.1016/j.bpa.2005.07.009